

Hierarchical Assembly of Collagen Peptide Triple Helices into Curved Disks and Metal Ion-Promoted Hollow Spheres

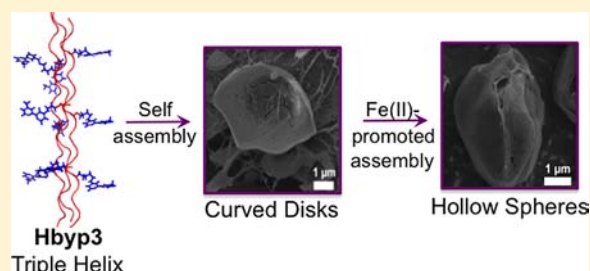
David E. Przybyla,[†] Charles M. Rubert Pérez,[†] Jeremy Gleaton,[†] Vikas Nandwana,[‡] and Jean Chmielewski^{*†}

[†]Department of Chemistry, Purdue University, 560 Oval Drive, West Lafayette, Indiana 47907, United States

[‡]Department of Chemistry, University of Massachusetts, Amherst, 710 North Pleasant Street, Amherst Massachusetts 01003, United States

S Supporting Information

ABSTRACT: A 27 amino acid collagen-based peptide (**Hbyp3**) was designed to radially display nine hydrophobic bipyridine moieties from a triple helical scaffold. Self-assembly of such functionalized triple helices led to the formation of micrometer-scaled disks with a curved morphology, presumably mediated by aromatic interactions, with a height that is in the range of the length of the triple helical peptide. Higher order assembly of these curved disks into micrometer-sized hollow spheres was accomplished through metal–ligand interactions between bipyridine groups of the disks and metal ions such as Fe(II), Co(II), Zn(II) and Cu(II). The thickness of the shell of these hollow spheres corresponds well with the thickness of the collagen peptide-based triple helix and the corresponding self-assembled disks. Addition of a metal ion chelator was found to reverse the assembly of the hollow spheres back to the curved disk structures. These data support the formation of the hollow spheres from the self-assembled disks of **Hbyp3** upon addition of metal ions.



INTRODUCTION

Designed hierarchical assembly of biopolymers into nano- and micro-scaled supramolecular structures is an area of interest for a range of applications such as biomedical imaging, drug delivery and tissue engineering.¹ For instance, re-engineering naturally occurring proteins such as the homohexameric Hcp1 from *Pseudomonas aeruginosa* results in the formation of protein nanotubes,² whereas nano-scale cages have been designed de novo by engineering self-assembling protein interactions.³ The design of α - and β -amino acid peptides^{1c,4,5} and peptoids⁶ containing discrete self-assembly signals has led to a number of higher-order structures, including fibers, ribbons, sheets, nanospheres and nanorings.

Designed collagen-based peptides have been found to self-assemble into a variety of supramolecular nano- to micro-structures. For instance, fibrils and fibers have resulted from use of a modified cysteine knot,⁷ π - π stacking,⁸ cation- π interactions,⁹ metal–ligand interactions,¹⁰ electrostatic interactions^{11,12} and metal-mediated coassembly,¹³ the latter two forming a banding pattern within the fibrils that is reminiscent of natural collagen. Hollow microtubules have been generated from collagen-like peptides¹⁴ and biotin–avidin interactions have been integrated with collagen peptides to generate films.¹⁵ Collagen peptide-based microflorettes and three-dimensional meshes have also resulted from harnessing metal–ligand interactions.¹⁶ In a recent report, a collagen-based peptide modified with two bipyridine moieties was found to assemble into 50–500 nm disks through Fe(II)-promoted radial

assembly.¹⁷ However, prior to the addition of the metal ion, poorly defined aggregates (~ 75 nm) were observed with this system.

In an effort to strengthen potential aromatic interactions between triple helices in a radial fashion, we designed a peptide that contained repeating units of proline-hydroxyproline-glycine (Pro-Hyp-Gly, POG) with an increased number of aromatic groups per triple helix (**Hbyp3**, Figure 1). We

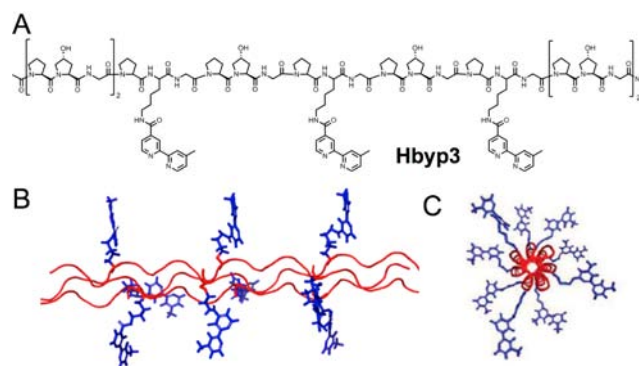


Figure 1. (A) Sequence of the collagen-based peptide **Hbyp3** containing three central bipyridine ligands. Schematic representation of the triple helix of **Hbyp3** from (B) a side view and (C) from above.

Received: August 2, 2012

Published: February 12, 2013

speculated that a triple helix containing nine radially displayed bipyridine units may undergo association in the absence of metal ions. Such an assembly may have the potential to be trapped with metal ions. Herein we disclose the hierarchical assembly of triple helices of **Hbyp3** first into micrometer-sized disks, followed by metal-promoted assembly into hollow spheres.

RESULTS AND DISCUSSION

The **Hbyp3** peptide was prepared using a previously described procedure.¹⁷ The circular dichroism spectrum for **Hbyp3** (250 μ M in 10 mM HEPES pH 7.0 buffer) displayed a maximum at 225 nm, a value that is consistent with a polyproline type II helix (Figure 2A). Thermal denaturation studies confirmed that

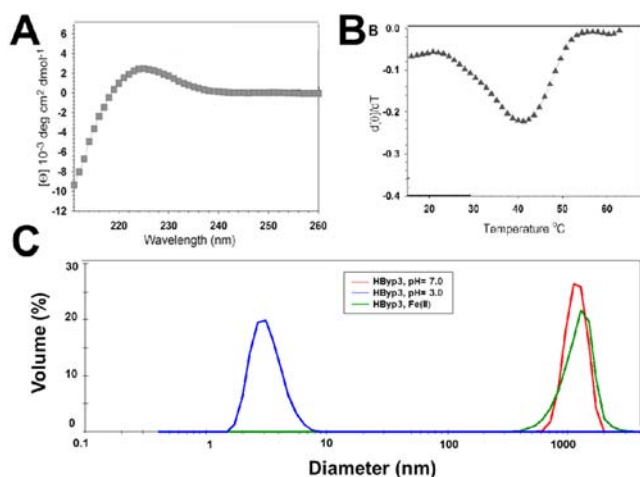


Figure 2. (A) CD spectroscopy of **Hbyp3** (250 μ M) in 10 mM HEPES pH 7.0. (B) First derivative ($d[\theta]/dT$) of the melting curve for **Hbyp3** (250 μ M). (C) Dynamic light scattering of **Hbyp3** (250 μ M) (red, 10 mM HEPES pH 7.0; blue, 10 mM glycine pH 3.0) and with $\text{Fe}(\text{ClO}_4)_2$ (250 μ M) (green) in 10 mM HEPES pH 7.0.

Hbyp3 formed a stable triple helix in aqueous solution with a melting temperature (T_m) of 42 $^{\circ}\text{C}$ (Figure 2B). The addition of three bipyridines to the POG core of the peptide was found to significantly lower the stability of the triple helix as compared to an unfunctionalized POG₉ peptide ($T_m \sim 70$ $^{\circ}\text{C}$). However, the triple helix stability for **Hbyp3** was slightly increased as compared to a collagen peptide containing only two bipyridine moieties (**Hbyp2**, T_m of 39 $^{\circ}\text{C}$),¹⁷ potentially due to additional supramolecular assembly from the bipyridines.

To probe this assembly issue, dynamic light scattering (DLS) experiments were performed on solutions of **Hbyp3** (250 μ M, 10 mM HEPES pH 7.0 buffer) that were thermally annealed (80 $^{\circ}\text{C}$ for 30 min, 4 $^{\circ}\text{C}$ for 48 h). Large assemblies were observed by DLS with a diameter of approximately 1100 nm (Figure 2C). To determine if the triple helix stability of **Hbyp3** was linked to the formation of these higher order assemblies, we also performed the CD and DLS experiments at pH 3 to protonate the bipyridine groups and potentially disrupt association. In this case, only smaller particles (~ 3 nm) were observed by DLS (Figure 2C), a value that has been previously reported for collagen peptide triple helices of this size.^{10,17} This shift in the assembly from large particle sizes at pH 7 toward triple helices at pH 3, however, had little effect on the T_m of the triple helix of **Hbyp3** as measured by CD (42 $^{\circ}\text{C}$). These data indicate that the triple helix plays a dominant role in the

stability of the structure as opposed to further supramolecular assembly.

Atomic force microscopy (AFM) was used to image the morphology of these assembled species derived from **Hbyp3**. The AFM data showed circular structures in the range of 0.5–1.5 μ m in diameter (Figure 3A), with a height of ~ 11 nm

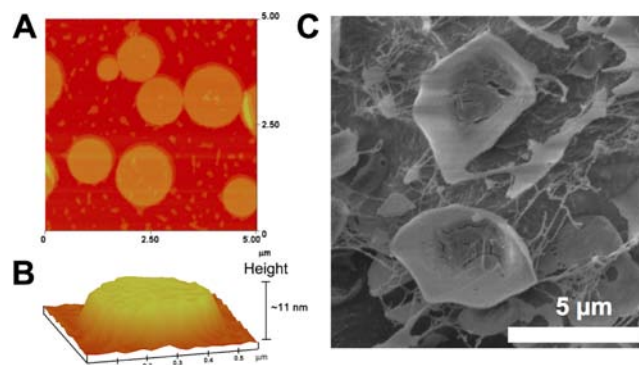


Figure 3. (A) AFM image of the assembled structure of **Hbyp3** (250 μ M in 10 mM HEPES pH 7.0 buffer) from the top and (B) the side. (C) Cryo-SEM image of the same sample.

(Figure 3B). This height corresponds well with the length of the triple helix that would form from **Hbyp3**. To more fully visualize the hydrated structures of the **Hbyp3** assemblies, we turned to cryo-scanning electron microscopy (SEM). Indeed obvious disk-like structures were observed, but with a curved morphology (Figure 3C). The thickness of these curved disks was measured to be in the range of approximately 12–16 nm. This increase in the height of the disks as compared to that found by AFM may be due to a more significant hydration of the curved disks in the cryo-SEM samples.

In an effort to probe the molecular packing and overall assembly within the disks of **Hbyp3**, we turned to wide- and small-angle X-ray scattering studies (WAXS and SAXS, respectively). WAXS data for the disk structures of **Hbyp3** showed a major peak at 5.9 $^{\circ}$, corresponding to d -spacing of 14.9 \AA (Figure 4A, blue). Broad peaks were also observed at

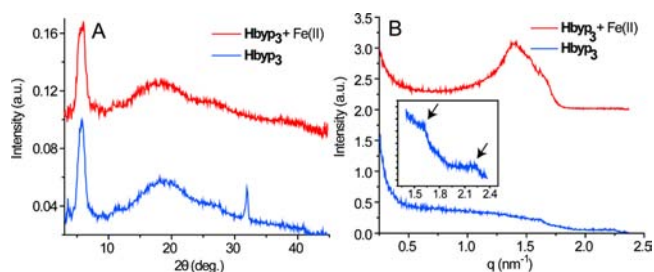


Figure 4. (A) WAXS and (B) SAXS profiles of **Hbyp3** assemblies (250 μ M) formed in 10 mM HEPES pH 7.0 buffer in absence (blue) and presence of $\text{Fe}(\text{ClO}_4)_2$ (red).

18.9 and 27.8 \AA , corresponding to d -spacing of 4.7 and 3.2 \AA . The larger d -spacing (14.9 \AA) is consistent with the reported diameter of a collagen peptide packed into a triple helical structure (15 \AA).¹⁸ The smaller d -spacing values in the WAXS pattern may be attributed to close packing of the bipyridine moieties (~ 3.5 –5 \AA). The sharp peak at 32 $^{\circ}$ is presumably artifactual. Analysis of the disk structures of **Hbyp3** by SAXS did not demonstrate strong scattering. However, two weak

peaks were observed at the wave vector (q) of 1.6 and 2.3 nm⁻¹ (Figure 4B, blue) that correspond to center-to-center spacing of 3.9 and 2.8 nm, respectively, suggesting a cubic assembly in the **Hbyp3** disks. These values are consistent with a model for cubic packed collagen peptide triple helices with interdigitating bipyridine units (Figure S3).

In the model for the self-assembly of **Hbyp3** triple helices into disks, supramolecular growth would be facilitated by aromatic interactions between bipyridine groups on neighboring triple helices. In this model the edges of the disks would be populated with available bipyridine ligands for metal ion coordination. Therefore, we evaluated the effect of added metal ions on the further assembly of the disk structures. A solution of **Hbyp3** (250 μM, 10 mM HEPES pH 7.0 buffer), that had been thermally annealed as described above to produce disks, was treated with Fe(ClO₄)₂ (250 μM). The off-white, disk precipitate turned dark pink immediately upon the addition of Fe(II). After 48 h, the precipitate was collected, washed with water, and analyzed by DLS. Large assemblies were observed by DLS with a diameter of approximately 1300 nm (Figure 2C). These assemblies were imaged by transmission electron microscopy (TEM) and AFM (Figure 5A,B). Both techniques

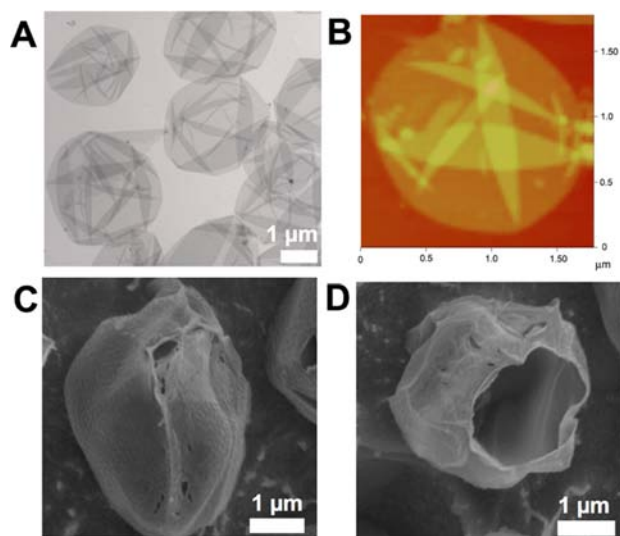


Figure 5. (A) TEM image of collapsed spheres resulting from metal ion-promoted assembly of disks of **Hbyp3** (250 μM, 10 mM HEPES pH 7.0 buffer) with Fe(ClO₄)₂ (250 μM), and (B) AFM image of the same sample. (C) Cryo-SEM image of the same spherical structures showing the seams along their length and (D) the hollow interiors.

provided evidence of rounded structures of about 1.5–3 μm that resembled collapsed spheres, where each fold in the material could be clearly seen. These structures show a striking resemblance to AFM images of hollow polymer shells from a layer-by-layer assembly process, followed by core decomposition.¹⁹ Upon increasing the amount of added Fe(II) to 1 mM, we found that very similar collapsed spheres formed by AFM (Figure S4).

Again we turned to cryo-SEM to more definitively image the hydrated morphology of the Fe(II)-promoted structures. The cryo-SEM images also displayed spherical structures of about 2–5 μm in diameter with pronounced seams along the length of the spheres (Figure 5C and Figure S5). Spheres that were situated at the face of the cryo sample were lacking a portion of their structure, potentially due to shearing from the microtome

during sample preparation (Figure 5D). These open spheres were found to be hollow with wall thicknesses of about 15–18 nm. WAXS analysis of the hollow spheres formed from **Hbyp3** and Fe(II) provided a very similar scattering pattern (Figure 4A, red) as that observed for the **Hbyp3** disks (Figure 4A). The 5.9° peak corresponding to a d -spacing of 14.9 Å, that was attributed to the triple helical structure, was maintained in the hollow spheres. SAXS analysis of the hollow sphere sample showed a strong peak at the wave vector 1.4 nm⁻¹, with a shoulder peak at 1.6 nm⁻¹ (Figure 4B, red). These values correspond to center-to-center distances of 4.5 and 3.9 nm, respectively, somewhat more elongated than in the disk structures, and still suggest cubic assembly. The emergence of the strong peak is most likely due to strong scattering from the metal ions in the sample. The disappearance of the peak at 2.3 nm⁻¹ that was observed in the disk structure indicates a change in the overall assembly of the sample due to metal–ligand interactions.

We investigated the effect of the added metal ion on higher order assembly of the hollow spheres. Addition of Co(ClO₄)₂, Zn(ClO₄)₂ or Cu(ClO₄)₂ (250 μM each) to the solution of **Hbyp3** disks described above again resulted in formation of the collapsed spheres (~1 μm) as imaged by TEM (Figure 6). The

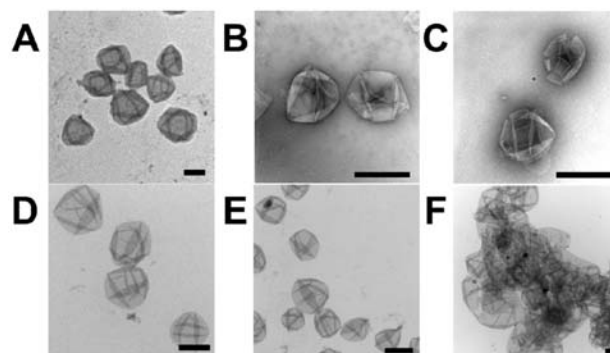


Figure 6. (A–E) Thermally annealed solutions of **Hbyp3** (250 μM) in HEPES pH 7.0 (10 mM) as described above were treated with 250 μM of the following metal ions (A) Co(ClO₄)₂, (B) Zn(ClO₄)₂, (C) Cu(ClO₄)₂, (D) CoSO₄, and (E) CoCl₂ and imaged by TEM. (F) A nonthermally annealed solution of **Hbyp3** (250 μM) in HEPES pH 7.0 (10 mM) was treated with Fe(ClO₄)₂ (250 μM) and imaged by TEM. Scale bars = 1 μm.

hollow spheres of the Cu(II) sample were found to be somewhat more fragile, however, and were observed to shatter more easily. This may be due to the propensity of Cu(II) to form weaker pentacoordinated complexes with bipyridine ligands and water.²⁰ We also investigated the role of the counterion on the formation of the hollow spheres with **Hbyp3**. For Co(II)-promoted hollow sphere assembly, very similar supramolecular structures were observed with perchlorate, sulfate and chloride ions (Figure 6D and E). The role of thermal annealing of solution of **Hbyp3** on the formation of hollow spheres was also probed (Figure 6F). Interestingly, **Hbyp3** samples that were not thermally annealed, but were mixed directly with Fe(ClO₄)₂, resulted in a highly irregular assembly with congealed and overlapping spheres. These data point to the importance of forming well ordered disks for the successful formation of the hollow spheres upon the addition of metal ions.

In an effort to probe the mechanism of the formation of hollow spheres from **Hbyp3**, we followed the progress of the

sphere-forming reaction. The collapsed sphere-like structures were visible by AFM even 1 min after the addition of Fe(II), with disks also observed. After 1 h, the spheres were the dominant species in the mixture (Figure S6). The sphere-forming reaction was also imaged using cryo-SEM immediately following the addition of Fe(II). This analysis showed a number of incomplete spheres (spheres missing one or more panels) at this early time point (Figure 7A and Figure S7). Since the

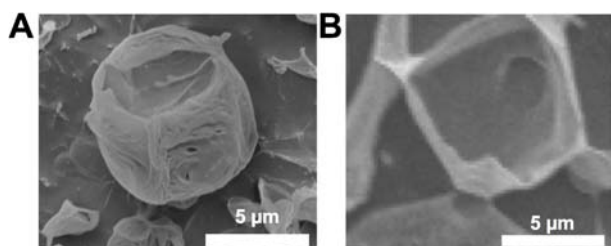


Figure 7. (A) Cryo-SEM image of the Fe(II)-promoted (250 μ M) assembly of Hbyp3 (250 μ M in 10 mM HEPES pH 7.0 buffer) after 1 min. (B) Cryo-SEM image after addition of EDTA (250 μ M, 30 min) to the preformed Fe(II)-Hbyp3 hollow spheres.

hollow spheres were formed upon addition of metal ions, presumably due to metal–ligand interactions, it should be possible to remove the metal ions from the assembly. With this in mind, we added EDTA (250 μ M, 30 min) to chelate the metal ions of the preformed spheres. Cryo-SEM imaging of the resulting material resulted in the observation of a number of disk-like structures (Figure 7B and Figure S8). In total, these data support the direct formation of the hollow spheres from the self-assembled disks of Hbyp3 upon addition of metal ions, potentially mediated by interactions between bipyridine ligands on the periphery of the disks and the metal ions.

CONCLUSION

Examples of self-assembling, nanoscale polypeptide cages abound in nature, from viral particles to protein shells of ferritin and heat shock proteins.²¹ Virus capsid assembly, for instance, is commonly a stepwise process that starts with protein assembly into larger building blocks, which then assemble into virus capsids.²² In this work, we describe a 27 amino acid peptide that first self-assembles into a triple helix and micrometer-sized disks. These disks then fuse together in a metal ion-dependent fashion into spherical shells that are about two-orders of magnitude larger than the protein cages found in nature. Sphere-like hollow assemblies in nature usually encapsulate matter, such as DNA and RNA within virus capsids or iron cores within a ferritin cage. Designed surface modifications of protein assemblies have shown promise,²³ such as chemically modifying cowpea mosaic virus nanoparticles with RGD peptides for selective cancer cell affinity,²⁴ and dual modification of bacteriophage MS2 viral capsids for targeted photodynamic therapy.²⁵ Future studies will focus on encapsulation and surface modification strategies with these collagen peptide-based hollow spheres.

ASSOCIATED CONTENT

Supporting Information

Experimental procedures, characterization, CD and microscopy data. This material is available free of charge via the Internet at <http://pubs.acs.org>.

AUTHOR INFORMATION

Corresponding Author

chml@purdue.edu

Notes

The authors declare no competing financial interest.

ACKNOWLEDGMENTS

We are grateful to NSF (0848325-CHE and 1213948-CHE) and the TRASK Foundation for support of this research, and to D. Sherman for assistance with SEM and TEM and Vince Rotello for helpful discussions.

REFERENCES

- (1) (a) Rabotyagova, O. S.; Cebe, P.; Kaplan, D. L. *Biomacromolecules* **2011**, *12*, 269. (b) Howorka, S. *Curr. Opin. Biotechnol.* **2011**, *22*, 485. (c) Woolfson, D. N.; Mahmoud, Z. N. *Chem. Soc. Rev.* **2010**, *39*, 3464. (d) Branco, M. C.; Schneider, J. P. *Acta Biomater.* **2009**, *5*, 817. (e) Vandermeulen, G. W. M.; Klok, H. A. *Macromol. Biosci.* **2004**, *4*, 383. (f) Brodin, J. D.; Ambroggio, X. I.; Tang, C.; Parent, K. N.; Baker, T. S.; Tezcan, F. A. *Nature Chem.* **2012**, *4*, 375.
- (2) Ballister, E. R.; Lai, A. H.; Zuckermann, R. N.; Cheng, Y.; Mougous, J. D. *Proc. Natl. Acad. Sci. U.S.A.* **2008**, *105*, 3733.
- (3) (a) Lai, Y.-T.; Cascio, D.; Yeates, T. O. *Science* **2012**, *336*, 1129. (b) King, N. P.; Sheffler, W.; Sawaya, M. R.; Vollmar, B. S.; Sumida, J. P.; Andre, I.; Gonen, T.; Yeates, T. O.; Baker, D. *Science* **2012**, *336*, 1171.
- (4) (a) Zhou, M.; Bentley, D.; Ghosh, I. *J. Am. Chem. Soc.* **2004**, *126*, 734. (b) Lu, K.; Jacob, J.; Thiyagarajan, P.; Conticello, V. P.; David, L. G. *Biophys. J.* **2004**, *86*, 505a. (c) Percec, V.; Dulcey, A. E.; Balagurusamy, V. S.; Miura, Y.; Smidrkal, J.; Peterca, M.; Nummelin, S.; Edlund, U.; Hudson, S. D.; Heiney, P. A.; Duan, H.; Magonov, S. N.; Vinogradov, S. A. *Nature* **2004**, *430*, 764. (d) Fujimura, F.; Kimura, S. *Org. Lett.* **2007**, *9*, 793. (e) Murasato, K.; Matsuura, K.; Kimizuka, N. *Biomacromolecules* **2008**, *9*, 913. (f) Kushner, A. M.; Guan, Z. *Angew. Chem., Int. Ed.* **2011**, *50*, 9026 and references therein. (g) Hamley, I. W. *Angew. Chem., Int. Ed.* **2007**, *46*, 8128 and references therein. (h) Mart, R. J.; Osborne, R. D.; Stevens, M. M.; Ulijn, R. V. *Soft Matter* **2006**, *2*, 822 and references therein. (i) Gazit, E. *Chem. Soc. Rev.* **2007**, *36*, 1263 and references therein.
- (5) Pomerantz, W. C.; Yuwono, V. M.; Pizzey, C. L.; Hartgerink, J. D.; Abbott, N. L.; Gellman, S. H. *Angew. Chem., Int. Ed.* **2008**, *47*, 1241.
- (6) Sani, B.; Kudirka, R.; Cho, A.; Venkateswaran, N.; Oliver, G. K.; Olson, A. M.; Tran, H.; Rarada, R. M.; Tan, L.; Zuckermann, R. N. *J. Am. Chem. Soc.* **2011**, *133*, 20808.
- (7) (a) Kotch, F. W.; Raines, R. T. *Proc. Natl. Acad. Sci. U.S.A.* **2006**, *103*, 3028. (b) Koide, T.; Homma, D. L.; Asada, S.; Kitagawa, K. *Bioorg. Med. Chem. Lett.* **2005**, *15*, 5230. (c) Krishna, O. D.; Kiick, K. L. *Biomacromolecules* **2009**, *10*, 2626.
- (8) Cejas, M. A.; Kinney, W. A.; Chen, C.; Leo, G. C.; Tounge, B. A.; Vinter, J. G.; Joshi, P. P.; Maryanoff, B. E. *J. Am. Chem. Soc.* **2007**, *129*, 2202.
- (9) Chen, C. C.; Hsu, W.; Kao, T. C.; Horng, J. C. *Biochemistry* **2011**, *50*, 2381.
- (10) Przybyla, D. E.; Chmielewski, J. *J. Am. Chem. Soc.* **2008**, *130*, 12610.
- (11) O'Leary, L. E. R.; Fallas, J. A.; Bakota, E. L.; Kang, M. K.; Hartergrink, J. D. *Nat. Chem.* **2011**, *3*, 821.
- (12) Rele, S.; Song, Y.; Apkarian, R. P.; Qu, Z.; Conticello, V. P.; Chaikof, E. L. *J. Am. Chem. Soc.* **2007**, *129*, 14780.
- (13) Pires, M. M.; Przybyla, D. E.; Rubert Perez, C.; Chmielewski, J. *J. Am. Chem. Soc.* **2011**, *133*, 14469.
- (14) Reiner, A. E.; Feher, K. M.; Hernandez, D.; Slowinska, K. J. *Mater. Chem.* **2012**, *22*, 7701.
- (15) Matsui, S.; Yamazaki, C. M.; Koide, T. *Macromol. Rapid Commun.* **2012**, *33*, 911.

- (16) (a) Pires, M. M.; Chmielewski, J. *J. Am. Chem. Soc.* **2009**, *131*, 2706. (b) Pires, M. M.; Przybyla, D. E.; Chmielewski, J. *Angew. Chem., Int. Ed.* **2009**, *48*, 7813.
- (17) Przybyla, D. E.; Chmielewski, J. *J. Am. Chem. Soc.* **2010**, *132*, 7866.
- (18) Xu, F.; Jain, V.; Tu, R. S.; Huang, Q.; Nanda, V. *J. Am. Chem. Soc.* **2012**, *134*, 47.
- (19) Donath, E.; Sukhorukov, G. B.; Caruso, F.; Davis, S. A.; Mohwald, H. *Angew. Chem., Int. Ed. Engl.* **1998**, *37*, 2202.
- (20) Martell, A. E. *Critical Stability Constants*; Plenum Press: New York, 1975; Vol. 2.
- (21) Lee, L. A.; Wang, Q. *Nanomed. Nanotechnol. Biol. Med.* **2006**, *2*, 137.
- (22) Zlotnick, A.; Mukhopadhyay, S. *Trends Microbiol.* **2011**, *19*, 14.
- (23) (a) Lee, L. A.; Huong, G. N.; Wang, Q. *Org. Biomol. Chem.* **2011**, *9*, 6189. (b) Pokorski, J. K.; Steinmetz, N. F. *Mol. Pharmaceutics* **2011**, *8*, 29. (c) Dedeo, M. T.; Finley, D. T.; Francis, M. B. *Prog. Mol. Biol. Transl. Sci.* **2011**, *103*, 353.
- (24) Hovlid, M. L.; Steinmetz, N. F.; Laufer, B.; Lau, J. L.; Kuzelka, J.; Wang, Q.; Hyypiä, T.; Nemerow, G. R.; Kessler, H.; Manchester, M.; Finn, M. G. *Nanoscale* **2012**, *4*, 3698.
- (25) Stephanopoulos, N.; Tong, G. J.; Hsiao, S. C.; Francis, M. B. *ACS Nano* **2010**, *4*, 6014.